Int. J. Therm. Sci. (2001) 40, 82–93

S1290-0729(00)01182-0/FLA

Natural convection in a confined saturated porous medium with horizontal temperature and vertical solutal gradients

Abdulmajeed A. Mohamad [a]*, Rachid Bennacer [b]

[a] *Department of Mechanical and Manufacturing Engineering, University of Calgary, Calgary, T2N 1N4, Canada*

[b] *IUSI, rue d'Eragny, 95031 Neuville-sur-Oise, France*

(Received 15 July 1999, accepted 2 February 2000)

Abstract — Double-diffusive natural convection in a horizontal enclosure filled with saturated porous medium is investigated numerically. Brinkman extension of Darcy model is adopted in the analysis. The enclosure is heated and cooled along vertical walls and solutal gradient is imposed vertically. The objective of the work is to understand the physics of the flow and to identify the flow regimes for thermal and solutal dominated flows. Since the number of parameters is large, the results are reported for an aspect ratio of two, Prandtl number of 0.71 (air) and Lewis number of 10 (hydrocarbon fuel). Grashof and Darcy numbers may vary between 10^6–10^8 and 10^{-4}–10^{-6}, respectively. It is found that the flow becomes unstable for finite range of solutal-to-thermal buoyancy ratio and it is possible to obtain different solutions in this region, depending on the initial condition. Funnel-type channelling flow is predicted along the vertical boundaries for thermally driven flow. Also, for thermally driven flow, concentration reversal is possible due to the thermal advection mechanism. Strong stratified fluid may suppress the thermal convection and heat transfer becomes conductive. © 2001 Éditions scientifiques et médicales Elsevier SAS

double diffusive natural convection / porous medium / modelling / thermal and solutal flow

Nomenclature

A	aspect ratio $= L/H$	
C	dimensional solute concentration	
D	effective mass diffusivity	$m^2 \cdot s^{-1}$
Da	Darcy number $= K/H^2$	
g	gravitational acceleration	$m \cdot s^{-2}$
Gr_T	thermal Grashof number $= g\beta_T \Delta T H^3/\nu^2$	
Gr_m	modified Grashof number $= Gr\,Da$	
H, L	height and length of the enclosure	m
K	permeability of the porous medium	m^2
Le	effective Lewis number $= \alpha/D$	
N	buoyancy ratio $= \beta_S \Delta C/\beta_T \Delta T$	
Nu	average Nusselt number	
P	dimensionless pressure	
Pr	effective Prandtl number $= \nu/\alpha$	
Sc	effective Schmidt number $= \nu/D$	
Sh	average Sherwood number	
T	dimensional temperature	K
u (v)	horizontal (vertical) components of the velocity	
U (V)	horizontal (vertical) dimensionless components of velocity $= uH/\nu$ (vH/ν)	
x, y	coordinate system	m

Greek symbols

α	effective thermal diffusivity	$m^2 \cdot s^{-1}$
β_S	coefficient of density change due to concentration	
β_T	coefficient of volumetric thermal expansion	K^{-1}
ε	porosity	
η (ξ)	dimensionless coordinate system $= y/H$ (x/H)	
ϕ	dimensionless concentration $= (C - C_0)/\Delta C$	
θ	dimensionless temperature $= (T - T_c)/\Delta T$	
ΔC	concentration difference between horizontal boundaries $= C_1 - C_0$	
ΔT	temperature difference between vertical boundaries $= T_h - T_c$	
ν	effective kinematic viscosity	$m^2 \cdot s^{-1}$
ρ	fluid density	$kg \cdot m^{-3}$

Subscripts

l	high
c	cold
h	hot

* Correspondence and reprints.
E-mail address: amohamad@enme.ucalgary.ca (A.A. Mohamad).

0 reference state
S solutal
T thermal

1. INTRODUCTION

Double-diffusive natural convection in a saturated porous medium in an enclosure stimulates a variety of applications, such as food processing, grain storage installation, electrochemical processes, underground spreading of pollutants, geophysical systems, etc. A comprehensive review of the literature on double-diffusive natural convection in a saturated porous medium can be found in [1–5]. Two kinds of problems have been considered in the literature: heat and mass gradients are imposed horizontally along the enclosure (aid or opposing each other) and heat and mass gradients are imposed vertically along the height of the enclosure (modified Rayleigh–Bénard convection). The first kind has been considered by Trevisan and Bejan [1, 6], Alavyoon [3], Mamou et al. [4, 7], Nithiarasu et al. [5, 8], Goyeau et al. [9], Karimi-Fard et al. [10] and recently by Mamou et al. [11] for different boundary conditions. Numerical and theoretical analysis have been considered by the mentioned authors for a range of Gr_m, *Le*, buoyancy ratio (N) for aiding and opposing conditions.

The second kind of problem was considered by [11–14]. Trevisan and Bejan [13] performed theoretical and numerical analysis for a problem of heat and mass transfer in a saturated porous layer heated from below with vertical mass concentration, where the flow is assumed to be thermally driven. Chen and Chen [15] considered unsteady solution for the same problem and they identified different flow regimes. Heating an enclosure from below with vertically imposed concentration gradient (stably or unstably solutally stratified fluid) is mostly unstable and three-dimensional in nature, especially for relatively high Rayleigh numbers. Such a problem exhibits quite complex flow structure for Lewis number not equal to unity.

As far as authors' knowledge concerns, no work is cited on cross relation between temperature and solutal gradient (i.e. temperature (concentration) gradient imposed horizontally and concentration (temperature) imposed vertically) in a saturated porous medium, which is subject of this work. Bergman and Ungan [16], Kranenborg and Dijkstra [17], Tsitverblit [18] and Dijkstra and Kranenborg [19] reviewed work done in enclosures filled with pure fluid subjected to lateral heating and vertical solutal gradient. Layering phenomena are predicted and observed in the enclosure. Stable or unstable stratification takes place in an enclosure subjected to negative or positive solutal gradient, respectively. Stably stratified fluid (linear diffusive gradient in vertical direction with negative gradient) may suppress any perturbation on the initial or boundary conditions. Lateral heating of an enclosure filled with stably stratified (solutal) fluid forces the fluid particles to move horizontally in the core of the enclosure and vertically near the vertical boundaries. Hence, differentially heated cavity has a tendency to mix the fluid, while the solutal effect has a tendency to prevent such a mixing. Therefore, it is expected that the competition between stabilizing (solutal) force and destabilising (thermal) force produces complex flow pattern. Filling a cavity with a saturated porous medium adds hydraulic resistance and alters the flow mechanism. This problem has fundamental importance as well as application in geophysics and chemical deposition. For instance, near liquid fuel storage tanks, fuel leaks into soil. Heat source nearby the tank may induce convection and reduce safety measures of the storage system. Then understanding such a problem is important in safety analysis.

The paper focuses on the analysis of the flow, heat and mass transfer in a horizontal cavity of aspect ratios of two for a range of Grashof and Darcy number. Prandtl number is fixed to 0.7 and *Le* to 10. The work is concentrated on stable stratified flow. The Darcy–Brinkman model is adopted in the analysis.

2. MATHEMATICAL FORMULATION

The physical model and coordinate system are shown in *figure 1*. The geometry under consideration is a two-dimensional horizontal enclosure of height H and width L filled with saturated porous medium. The vertical walls of the enclosure are subjected to temperatures

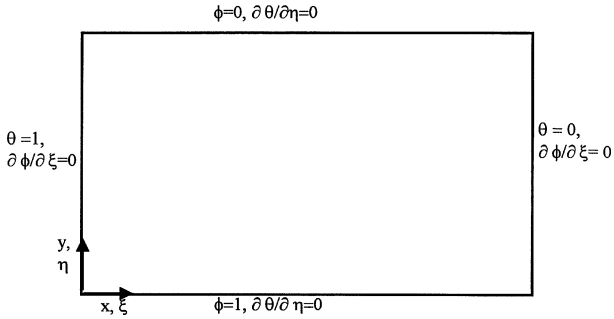

Figure 1. Schematic of the problem with coordinate system.

T_h and T_c at left and right walls, respectively. The horizontal walls are subjected to fixed concentrations, high concentration at the bottom (C_1) and low concentration (C_0) at the top of the enclosure. It is assumed that the flow is incompressible, steady and laminar and that the binary fluid is Newtonian. The thermophysical proprieties of the fluid are assumed to be constant, except density variation in the buoyancy term, which depends linearly on both the local temperature and concentration, i.e. Boussinesq approximation is assumed to be valid,

$$\rho(T,C) = \rho_0\left[1 - \beta_T(T - T_0) - \beta_S(C - C_0)\right] \quad (1)$$

where

$$\beta_T = -\frac{1}{\rho_0}\left[\frac{\partial\rho}{\partial T}\right]_C \quad \text{and} \quad \beta_S = -\frac{1}{\rho_0}\left[\frac{\partial\rho}{\partial C}\right]_T$$

Soret and Dufour effects on heat and mass diffusion are neglected. The solid matrix is supposed to be indeformable and in thermal equilibrium with the fluid. The permeability of the porous medium is uniform.

The height of the cavity (H) is taken as the reference length for the spatial coordinates ($\xi = x/H$ and $\eta = y/H$). The reference variables for velocity, pressure, temperature and species concentration are H^2/ν, ν/H, $\rho\nu^2/H^2$, ΔT and ΔC, respectively.

The Darcy–Brinkman formulation is adopted in the analysis. The dimensionless macroscopic conservation equations of mass, momentum, energy and species can be written as follows.

- *Continuity:*

$$\frac{\partial U}{\partial\xi} + \frac{\partial V}{\partial\eta} = 0 \quad (2)$$

- *Momentum:*

$$U\frac{\partial U}{\partial\xi} + V\frac{\partial U}{\partial\eta} = -\frac{\partial P}{\partial\xi} + \nabla^2 U - \frac{U}{Da} \quad (3a)$$

$$U\frac{\partial V}{\partial\xi} + V\frac{\partial V}{\partial\eta} = -\frac{\partial P}{\partial\eta} + \nabla^2 V - \frac{V}{Da} + Gr_T(\theta - N\phi) \quad (3b)$$

- *Energy:*

$$U\frac{\partial\theta}{\partial\xi} + V\frac{\partial\theta}{\partial\eta} = \frac{1}{Pr}\nabla^2\theta \quad (4)$$

- *Species transport equation:*

$$U\frac{\partial\phi}{\partial\xi} + V\frac{\partial\phi}{\partial\eta} = \frac{1}{Sc}\nabla^2\phi \quad (5)$$

The dimensionless parameters that characterize the problem are the aspect ratio of the cavity $A = H/L$, the Prandtl number $Pr = \nu/\alpha$, the Schmidt number $Sc = \nu/D$, the thermal Grashof number $Gr_T = (\beta_T g\Delta T H^3)/\nu^2$ and the buoyancy ratio N. The dimensionless parameter that characterizes the flow in porous media is the Darcy number $Da = K/H^2$.

Equation (3) represents the Darcy–Brinkman momentum equation, where the Forchheimer inertia term has been neglected. The analysis of Karimi-Fard et al. [10] showed that the inertial effect is almost negligible in double diffusive natural convection. Similar conclusions were drawn by Lauriat and Prasad [20].

The boundary conditions for the governing equations are non-slip conditions at the impermeable walls of the enclosure. The constant temperatures are assumed along vertical walls and adiabatic condition on the horizontal walls. The constant species concentrations are assumed along the horizontal walls and zero mass fluxes at the vertical walls of the enclosure. Hence,

$$U = V = 0, \quad \theta = 1, \quad \frac{\partial\phi}{\partial\xi} = 0 \quad \text{at } \xi = 0 \quad (6a)$$

$$U = V = 0, \quad \theta = 0, \quad \frac{\partial\phi}{\partial\xi} = 0 \quad \text{at } \xi = 2 \quad (6b)$$

$$U = V = 0, \quad \frac{\partial\theta}{\partial\eta} = 0, \quad \phi = 1 \quad \text{at } \eta = 0 \quad (6c)$$

$$U = V = 0, \quad \frac{\partial\theta}{\partial\eta} = 0, \quad \phi = 0 \quad \text{at } \eta = 1 \quad (6d)$$

The average rate of heat and mass transfer across the vertical and horizontal walls are expressed in dimensionless form by the Nusselt and Sherwood numbers:

$$Nu = \int_0^1 \left(\frac{\partial\theta}{\partial\xi}\right)_{\xi=0} d\eta \quad (7a)$$

$$Sh = \int_0^A \left(\frac{\partial\phi}{\partial\eta}\right)_{\eta=0} d\xi \quad (7b)$$

3. METHOD OF SOLUTION

A control volume, finite-difference approach is used to solve the model equations with specified boundary conditions. The SIMPLER algorithm is employed to solve the equations in primitive variables. Central differencing is used to approximate advection–diffusion terms, i.e. the scheme is second order accurate in space. The governing equations are converted into a system of algebraic equations through integration over each control volume. The algebraic equations are solved by a line-by-line iterative method. The method sweeps the domain of integration

along the x and y axes and uses tridiagonal matrix inversion algorithm to solve the system of equations. Fully implicit Euler method is used to march the solution in the time domain. Very large pseudo-time step is used to obtain the final converged solution. Velocity components are under-relaxed by a factor of 0.7 and temperature and solutal field are under-relaxed by a factor of 0.8 or 0.7. It is found that 4 000 iterations are sufficient to get convergent solution for most of the cases, some runs were carried up to 8 000 iterations. The criteria of convergence are to conserve mass, momentum, energy and species globally and locally, and to insure convergence of pre-selected dependent variables to constant values within machine error. It was difficult to get prescribed convergent criteria when the flow starts to fluctuate. These cases are discussed latter on.

In order to insure that the results are grid size independent, different meshes were tested, namely, 121×61, 161×81 and 201×101. The difference between predictions by using 121×61 and 161×81 grids was less than 1.3 % in *Nu*, *Sh*, maximum U and V velocity components at the mid plane of the enclosure. The difference between results obtained by using 161×81 and 201×101 grids was less than 0.7 %. The calculations are performed by adapting nonuniform 161×81 grids. Very fine grids are adopted near boundaries. The fine grids are necessary to resolve narrow channel flow, which is predicted for range of controlling parameters.

Furthermore, the code validation has been performed and compared with published results. Since there are no published results identified in the literature for cross thermal–solutal gradients, the boundary conditions are modified to reproduce the Goyeau et al. [9] results. *Table I* compares the present results with Goyeau's results for a square enclosure with cooperating thermal and solutal buoyancy forces and for $N = 0$. It can be seen that the agreement between the results is very good.

TABLE I
Comparison between present results and results of [9] for double diffusion in a square cavity with horizontal temperature and solutal gradients and for $N = 0$, $Pr = 10$, $Da = 10^{-5}$.

		Present results		Goyeau et al. [9]	
Gr_m	Le	Nu	Sh	Nu	Sh
10	10	3.102	13.34	3.11	13.25
10	100	3.102	42.42	3.11	41.53
100	10	13.50	49.12	13.47	48.32
100	100	13.50	146.20	13.47	140.65

4. RESULTS AND DISCUSSIONS

The controlling parameters that define the fluid flow and heat and mass transfers for double diffusive natural convection in an enclosure filled with a porous medium are the aspect ratio (A), Gr_T, N, Le and Da. It needs quite extensive analysis to cover effects of each parameter. It is intended to limit the analysis for Prandtl parameter of 0.71, $Le = 10$ and aspect ratio of two as a horizontal enclosure. It should be mentioned that Le for hydrocarbon fuels is between 2 and 5, but due to dispersion effect of porous medium, the effective Le may be increase. Hence, the effective Le is set to 10.

Stably stratified fluid prevents flow evolution. On the other hand, applying horizontal temperature gradient across the cavity initiates flow, even for very small temperature gradient. Hence, there is a competition between the thermal and solutal buoyancy forces. As N approaches zero, the thermal buoyancy drives the flow and formation of a longitudinal recirculated flow is expected for low and moderately high Gr_T numbers. As N becomes much larger than unity, the flow is suppressed in the enclosure and conduction dominates heat and mass transfer. Hence, the average Nusselt number approaches 0.5 and Sherwood number approaches 1.0 for aspect ratio of two, where the Nusselt and Sherwood numbers are based on the height of the enclosure. For N of the order of unity, the competition between the thermal and solutal buoyancy forces becomes of the same order. Within this range of N, the dynamic of the flow becomes more involved. Accordingly, the analysis is focused on this range of parameter N, i.e. N of the order of unity, specifically $0.25 \leq N \leq 2.0$. It should be mentioned that the solution started with stagnant initial condition unless otherwise stated.

The flow, thermal and species concentration structures are discussed first and then followed by discussion of the heat and mass transfer rates and bifurcation process.

4.1. Flow, isotherms and isoconcentrations distributions

The results are generated for $Gr_T = 10^6$, 10^7, 10^8 and for $Da = 10^{-4}$, 10^{-5}, 10^{-6} and for the above-mentioned range of the buoyancy forces ratio, N. It is found that the flow structure, isotherms and isoconcentrations are qualitatively the same for the same modified Grashof number Gr_m and for the same buoyancy ratio N. Hence, results are presented for $Gr_T = 10^8$ and for different

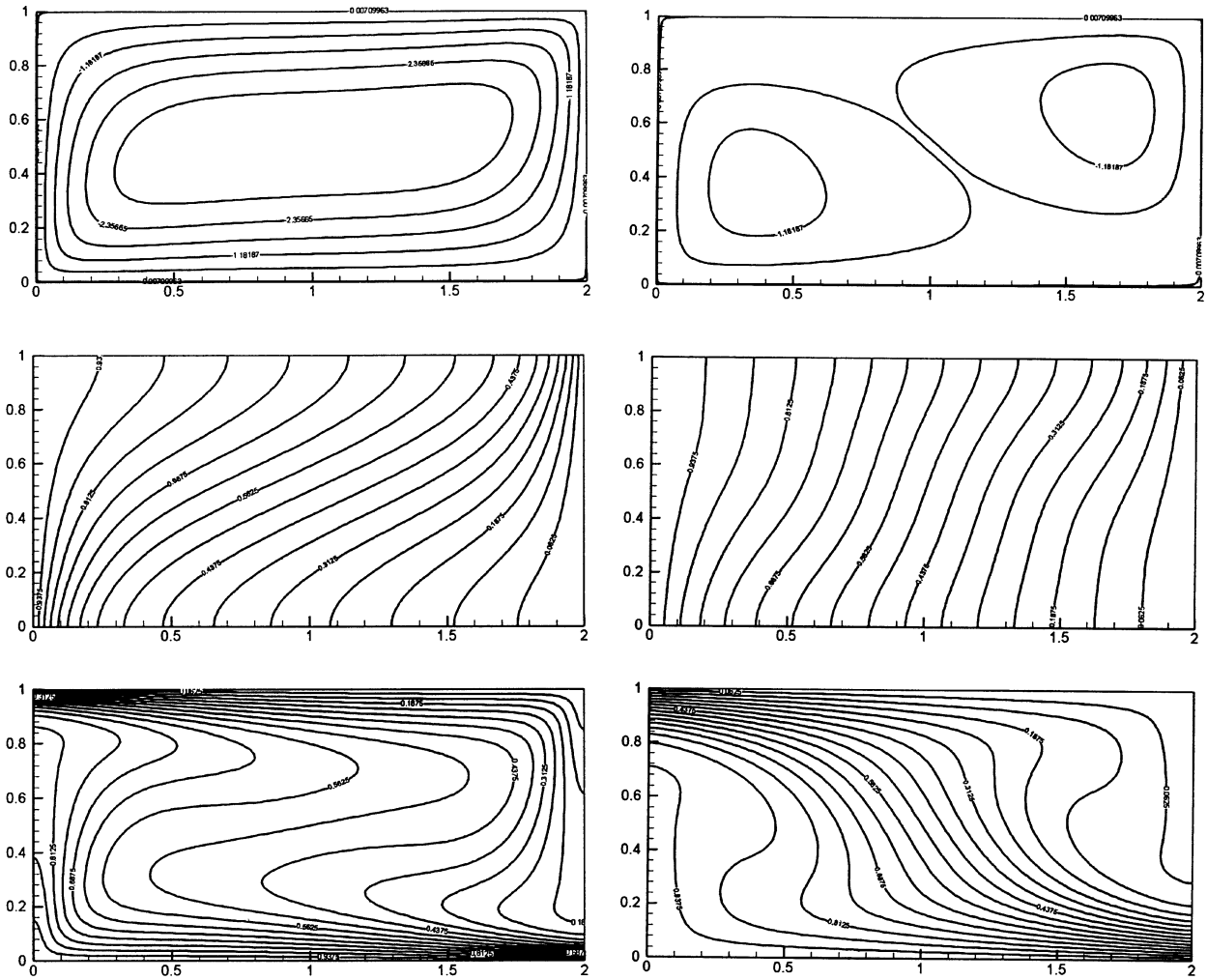

Figure 2. Streamlines (up), isotherms (middle) and isoconcentration lines (bottom) for $Gr_T = 10^8$, $Da = 10^{-6}$ ($Gr_m = 100$) for (a) $N = 0.25$, (b) $N = 0.8$, (c) $N = 1.0$ and (d) $N = 1.4$.

Darcy parameters, and the discussion may be valid for $Gr_T = 10^6$ and $Gr_T = 10^7$ but for a given Gr_m.

For $Gr_m = 10$ ($Gr_T = 10^8$, $Da = 10^{-7}$) and for $0.25 \leq N \leq 2.0$, the flow is almost stagnant except at the vicinity of the confining walls. Hence, there is no need to discuss the low modified Grashof numbers results.

The results for $Gr_T = 10^8$ and $Da = 10^{-6}$ ($Gr_m = 100$) are shown in *figures 2(a)–(d)* for $N = 0.25$, 0.8, 1.0 and 1.4, respectively. For $N = 0.25$, the flow is driven mainly by thermal buoyancy force. The flow structure consists of one main circulation in the entire enclosure. The concentration gradient reversal is evident at the core of the cavity, due to the strong flow recirculation. The isotherms reveal that the rate of heat transfer is high at the bottom of the hot wall (due to symmetry of the problem, at the upper part of the cold wall) due to flow impingement at this location, and rate of heat transfer decreases along the hot wall. As N value increases the strength of the flow circulation decreases and the flow bifurcates into two weak circulations, *figure 2(b)*. The bifurcation phenomena will be discussed later on. In fact, for $N < 0.8$, heavy fluid particles (high concentration) that advected to the upper part of the enclosure reach the other end of the enclosure and form recirculation. The horizontal trajectory of the heavy fluid particles decreases as N increases

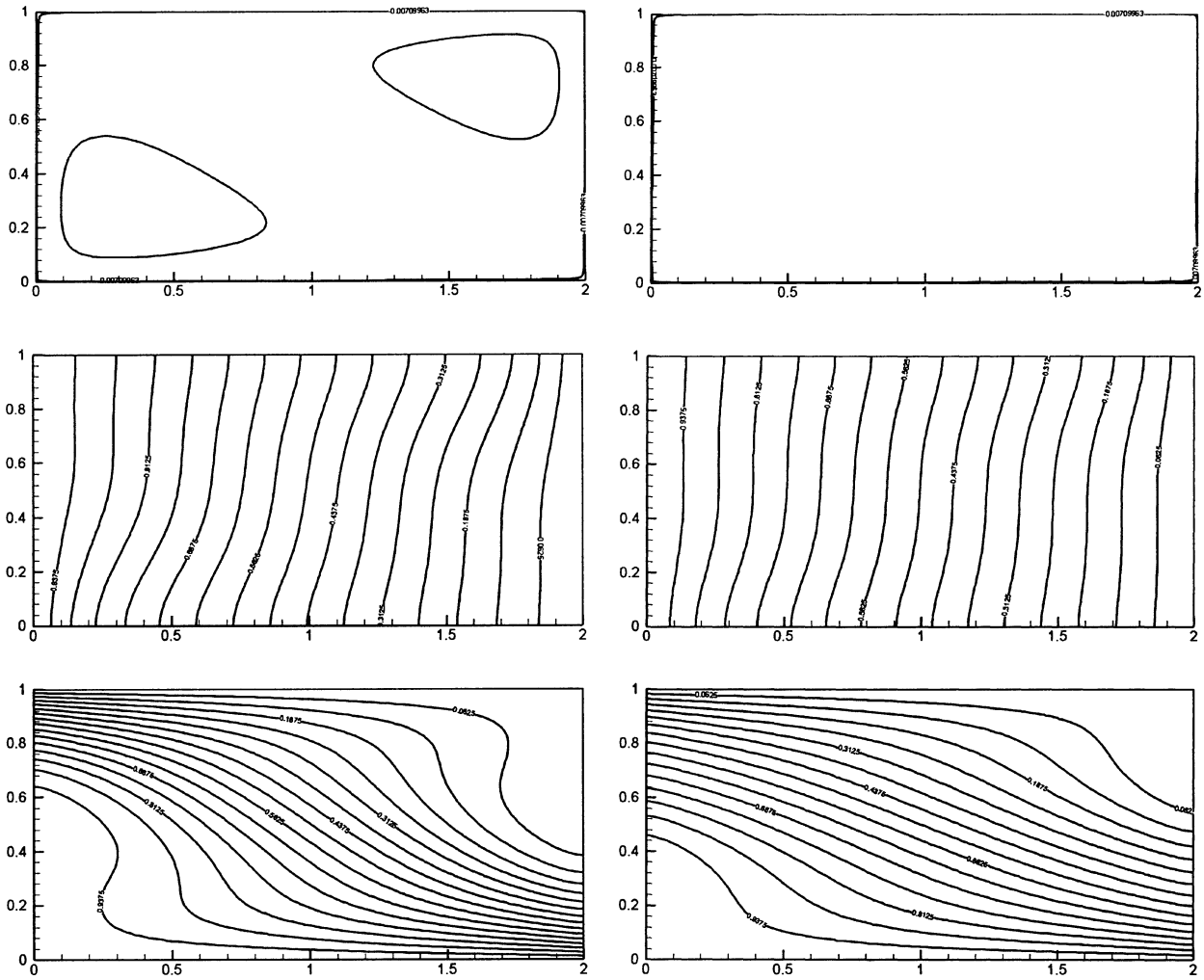

(c) (d)

Figure 2 (continued).

(stabilizing force). As N approaches 0.8, the heavy particles sink before they arrive at the other end of the enclosure forming two circulations. Also, the concentration reversal and isothermal distortion diminish as N increases. For $N = 1$ (*figure 2(c)*), the fluid in the core of the cavity becomes almost stagnant and flow channels along the boundaries. Heat transfer takes place mainly by conduction as is evident from the isotherm distribution. For $N = 1.4$ (*figure 2(d)*), a very weak flow channels along the boundaries and the fluid in the core is stagnant. The flow channeling has effect on the isoconcentration distributions at the left, bottom corner and due to centrosymmetry at the upper right corner. The flow channeling can be explained as follows: fluid particles adjacent to the vertical hot wall become hot and rise, while fluid particles away from the boundary gain heat by conduction and their temperature is less than the hot boundary temperature, hence, the flow is suppressed away from the hot boundary due to opposing solutal buoyancy. Since the solutal concentration decreases away from the bottom, the width of channel increases. Similar discussion can be applied for cold channel along the vertical cold boundary.

The medium becomes more permeable by increasing Darcy number. The results for $Da = 10^{-5}$ are given in *figure 3* for $Gr_T = 10^8$ ($Gr_m = 1\,000$). The flow structure

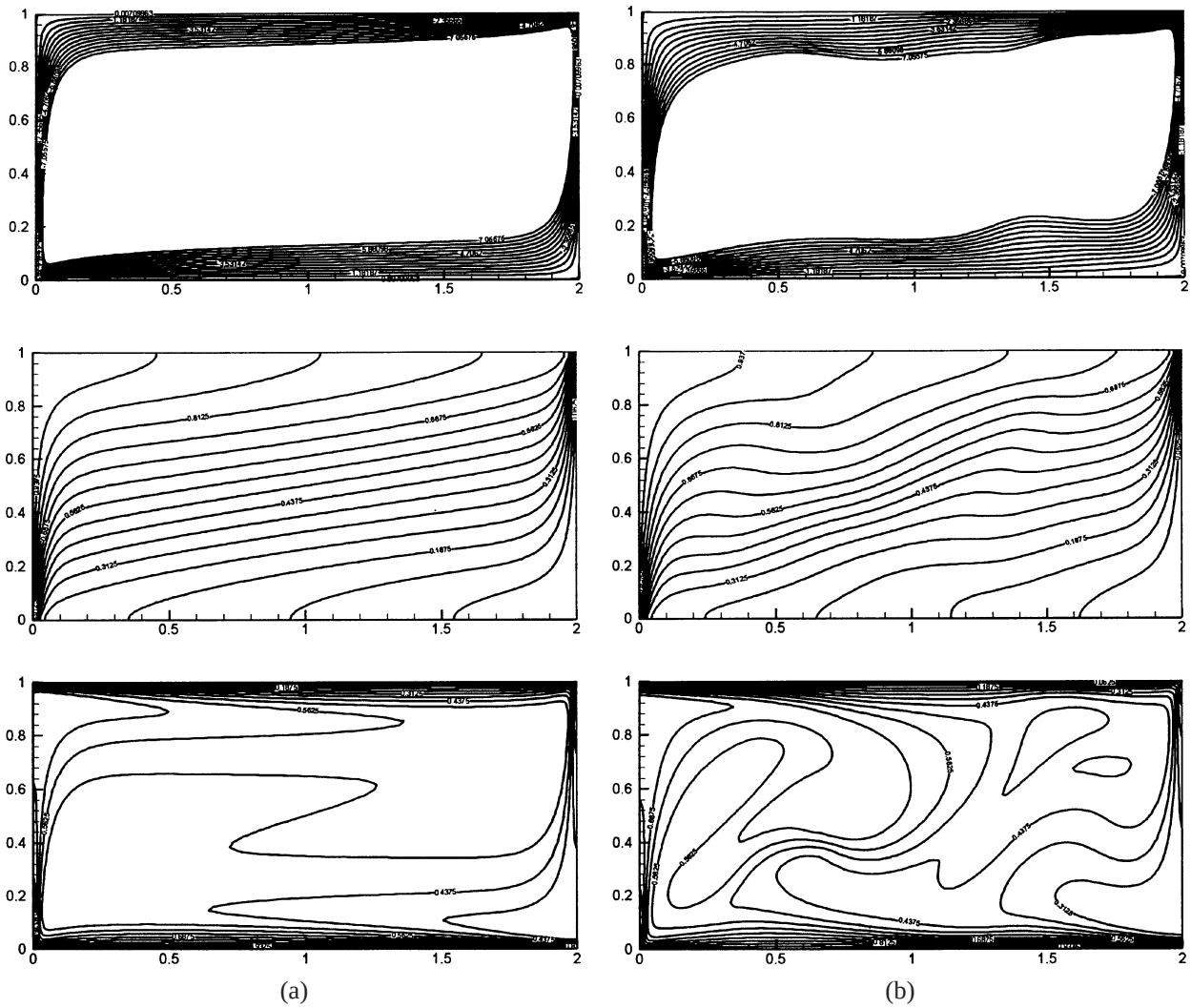

Figure 3. Streamlines (up), isotherms (middle) and isoconcentration lines (bottom) for $Gr_T = 10^8$, $Da = 10^{-5}$ ($Gr_m = 1\,000$) for (a) $N = 0.25$, (b) $N = 0.7$, (c) $N = 1.0$ and (d) $N = 2$.

is interesting, a strong flow channels along the boundaries, while the fluid in the core is almost stationary for $N = 0.25$ (*figure 3(a)*), where the flow is mainly driven by thermal buoyancy. This is due to formation of very thin thermal boundary layers along the heated and cooled boundaries. The thickness of the thermal boundary layer decreases as *Da* increases. Also, the concentration gradient reversal takes place due to high advective flow mechanism. Flow instability starts at $N = 0.7$, forming internal waves as evidenced in *figure 3(b)*. Steady state solution is not possible for $0.7 < N < 1.0$. The solution showed fluctuations from iteration to iteration. The fluctuation in *Nu* and *Sh* was about 10 % from iteration to iteration. For $N = 1.0$ (*figure 3(c)*), the flow bifurcated into two main recirculations at the left bottom corner and at the right upper corner, with weak multivortices between the two main recirculations. The distortion in the isotherms and isoconcentration lines are strong due to complex flow structure. As N increases ($N = 2.0$, *figure 3(d)*), the main circulations start to diminish in size and in strength and complex flow pattern forms with weak vortices. Heat transfer becomes mainly conductive for $N = 2.0$ (*figure 3(d)*). For increases in *Da* (10^{-4}) and for the same *Gr* as before

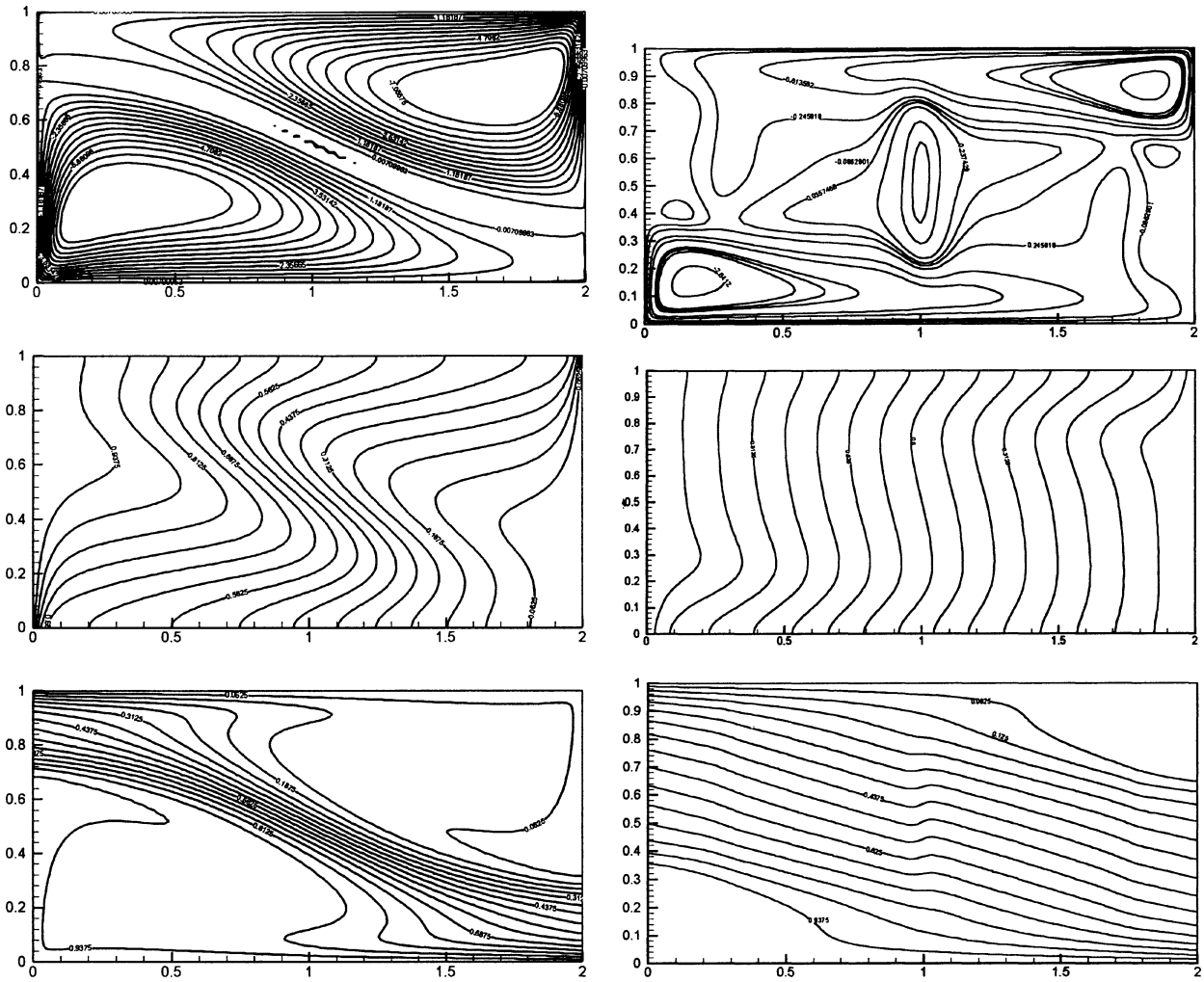

(c) (d)

Figure 3 (continued).

($Gr_T = 10^8$), the dynamics of the flow changes drastically. For thermally dominated flow, $N = 0.25$, a very narrow flow channels form along the boundaries, thermal stratification, solutal reversal and layering are evident in *figure 4(a)*. Similar flow, isotherm and iso-concentration structures remained until $N = 1.0$. At $N = 1.0$ (*figure 4(b)*), internal waves start to form along the horizontal boundaries. For $Gr_m = 10$, the flow is almost stagnant except at the vicinity of the confining walls for $0.25 \leq N \leq 2.0$, *figure 5*. Hence, there is no need to elaborate on these low modified Grashof number results.

4.2. Heat and mass transfer

Figures 5(a) and *5(b)* show Nusselt and Sherwood numbers as a function of N, respectively. The results are obtained by increasing N (starting from $N = 0.25$) after the convergence is achieved for a given Gr_m. Also, calculations are performed by decreasing N value after convergence is achieved for a given Gr_T, starting from $N = 1.4$ or higher value. The results for $Gr_m = 10$ indicate that the controlling parameter is modified Grashof number (Darcy regime). The heat transfer is mainly conductive for the range of N investigated. The rate of mass transfer increases by decreasing N, due

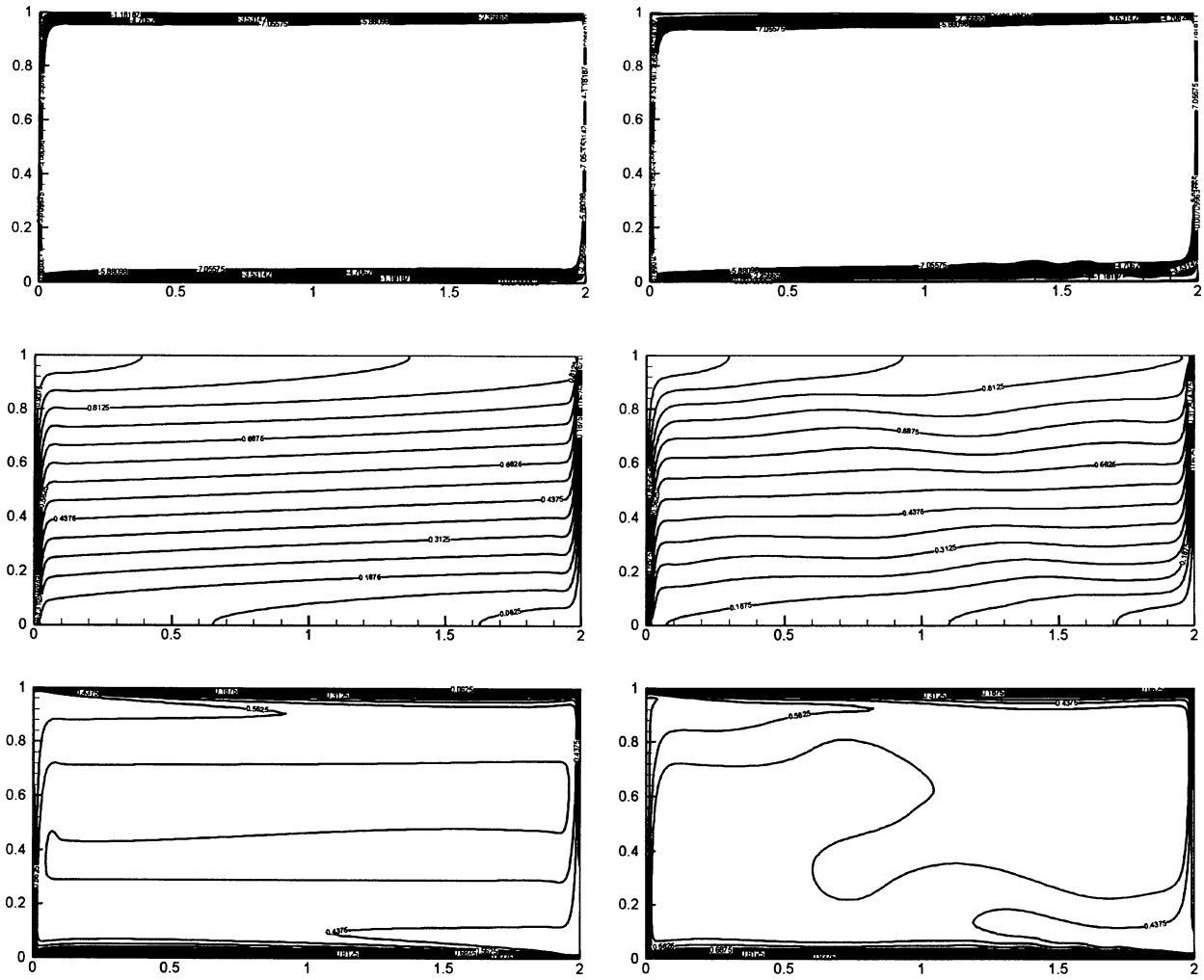

Figure 4. Streamlines (up), isotherms (middle) and isoconcentration lines (bottom) for $Gr_T = 10^8$, $Da = 10^{-4}$ ($Gr_m = 10\,000$) for (a) $N = 0.25$, and (b) $N = 1.0$.

to the advection mechanism induced by the thermal buoyancy.

For $Gr_m = 100$ and for $N > 0.7$, the controlling parameter is also Gr_m (Darcy regime). While, for $N < 0.7$, the controlling parameters are Gr_T and Da. The heat transfer becomes mainly conductive for $N > 1.4$ for $Gr_m = 100$. Mass transfer increases as N decreases, this is due to the effect of the thermal advection, which enhances the rate of mass transfer.

Figures 6(a) and *6(b)* show the Nusselt and Sherwood numbers as functions of N for $Gr_m = 1\,000$, respectively. It is interesting to notice multi-solution for $0.8 < N < 1.0$. In order to explain this phenomenon, reference is made to *figures 7(a)* and *7(b)* that are for the same $N = 0.88$. The results of *figure 7(a)* are produced by starting the solution from $N = 0.7$ as initial condition and N was increased stepwise after convergence solution is obtained for a given N value. Full convergence solution for $N = 0.88$ (starting from $N = 0.7$) was not possible, hence, the results of *figure 7(a)* are qualitative. *Figure 7(b)* is for $N = 0.88$ (as *figure 7(a)*), but the solution started from $N = 1.4$ (initial condition) and N was gradually decreased. This solution was then fully converged. Hence, the lower branch is stable and the upper branch is unstable (*figures 6(a)* and *6(b)*). The bifur-

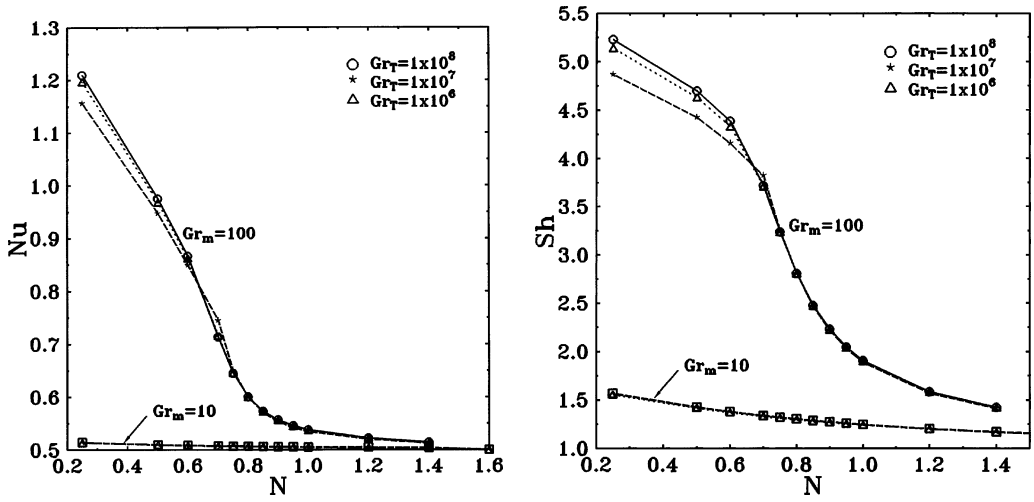

Figure 5. (a) Nusselt and (b) Sherwood parameters for $Gr_{\mathrm{m}} = 100$ and 10.

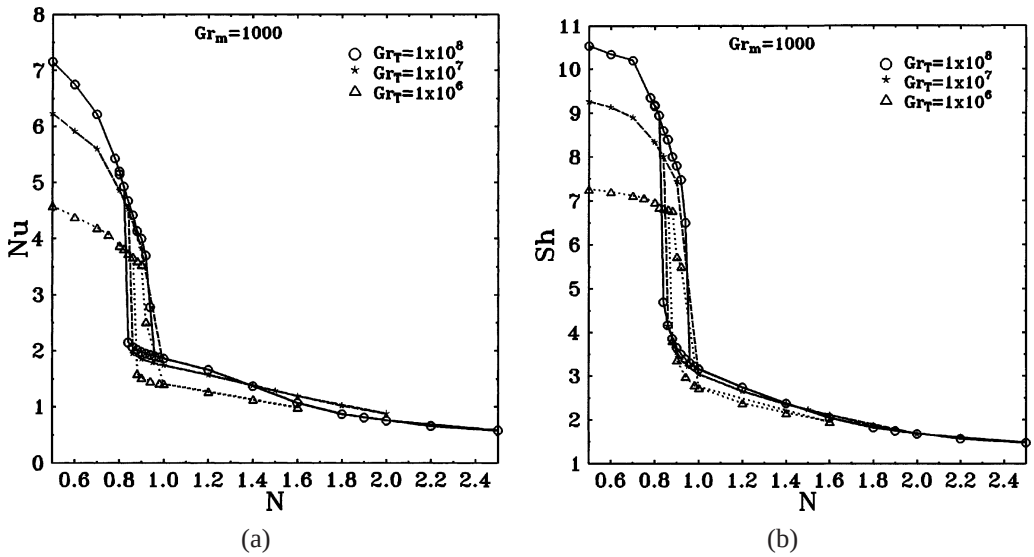

Figure 6. (a) Nusselt and (b) Sherwood parameters for $Gr_{\mathrm{m}} = 1\,000$.

cation can be explained as follows. When N increases from 0.25 (*figure 3(a)*) to 0.7 (*figure 3(b)*), the advected hot particles move toward the right-hand side and lose heat to adjacent particles, accordingly, their density increases. The particles start to sink into high concentration layer and retard forming internal wave (due to solutal reversal). The solutal reversal decreases as N increases, hence, the sinking particles do not suffer from retarding force. Accordingly, recirculation forms at the lower left corner. This discussion is also valid for the upper right-hand corner, due to skew symmetry of the problem. Also, it is evident from *figure 6(a)* that for $N > 1.6$, the controlling parameter is Gr_{m}. For $N > 2.4$ heat transfer is mainly conductive, where the flow is suppressed by stable solutal gradient. The results confirmed that as Gr_{m} increases N should be increased to suppress the thermal advection, i.e. heat transfer becomes conductive.

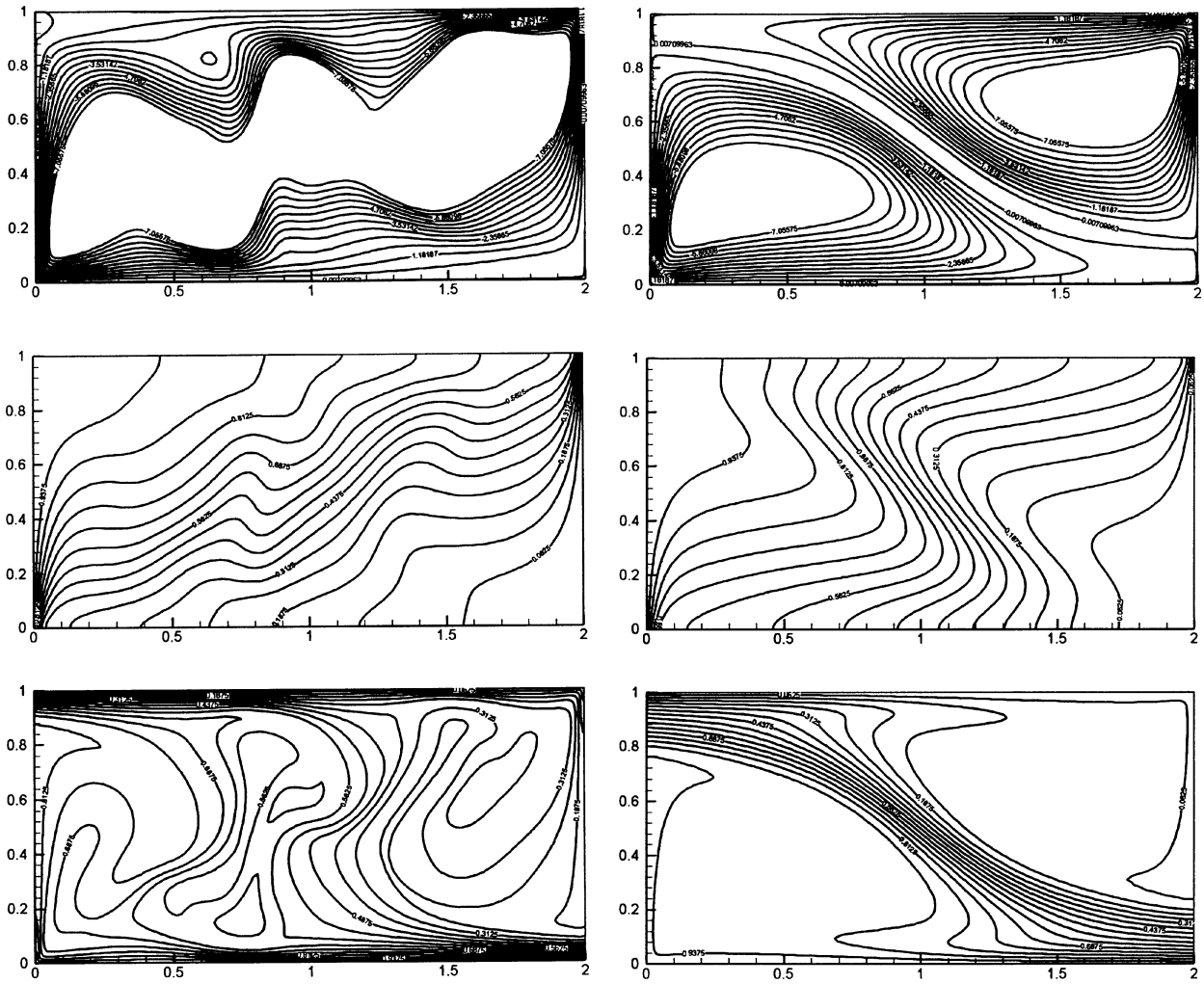

Figure 7. Streamlines, isotherms and isoconcentration lines for $Gr_m = 1\,000$ and $N = 0.88$, starting the solution from (a) lower and (b) higher N values.

5. CONCLUSIONS

Natural convection heat and mass transfer in a horizontal enclosure is investigated numerically. Temperature gradient is imposed horizontally while concentration gradient is imposed vertically. The flow structure and heat and mass transfer rates are discussed.

Flow channels along the vertical walls (as a funnel) for thermally driven flow due to suppression of the flow at the core of the enclosure by stabilization of species concentration. Also, solutal reversal is possible for thermally driven flow due to the advection mechanism.

The Darcy regime is predicted for $Gr_m = 10$ and also for $Gr_m = 100$ but for $N > 0.7$. Multiple solutions are possible for $Gr_m = 1\,000$ and for $0.8 \leq N \leq 1.0$. In this region bifurcation takes place from one main recirculating flow into two main recirculating flows. Also, it is evident that before the bifurcation occurs, internal waves form along the horizontal boundaries.

REFERENCES

[1] Trevisan O.V., Bejan A., Natural convection with combined heat and mass transfer buoyancy effects in a

porous medium, Int. J. Heat Mass Tran. 28 (1985) 1597–1611.

[2] Nield D.A., Bejan A., Convection in Porous Media, Springer, New York, 1992.

[3] Alavyoon F., On natural convection in vertical porous enclosures due to prescribed fluxes of heat and mass at the vertical boundaries, Int. J. Heat Mass Tran. 36 (1993) 2479–2498.

[4] Mamou M., Vasseur P., Bilgen E., Multiple solution for double-diffusive convection in a vertical porous enclosure, Int. J. Heat Mass Tran. 38 (1995) 1787–1798.

[5] Nishimura M., Wakamatsu M., Morega A.M., Oscillatory double-diffusive convection in a rectangular enclosure with combined horizontal temperature and concentrate ion gradients, Int. J. Heat Mass Tran. 41 (1998) 1601–1611.

[6] Trevisan O.V., Bejan A., Mass and heat transfer by natural convection in a vertical slot filled with porous medium, Int. J. Heat Mass Tran. 29 (1986) 403–415.

[7] Mamou M., Vasseur P., Bilgen E., Multiple solutions for double-diffusive convection in a vertical porous enclosure, Int. J. Heat Mass Tran. 38 (1995) 1787–1798.

[8] Nithiarasu P., Seetharamu K.N., Sundarajan T., Double-diffusive natural convection in an enclosure filled with fluid-saturated porous medium: A generalized non-Darcy approach, Numerical Heat Transfer A 30 (1996) 413–426.

[9] Goyeau B., Songbe J.-P., Gobin D., Numerical study of double-diffusive natural convection in a porous cavity using the Darcy–Brinkman formulation, Int. J. Heat Mass Tran. 39 (1996) 1363–1378.

[10] Karimi-Fard M., Charrier-Mojtabi M.C., Vafai K., Non-Darcian effects on double-diffusive convection within a porous medium, Numerical Heat Transfer A 31 (1997) 837–852.

[11] Mamou M., Vasseur P., Bilgen E., Double diffusive convection instability in a vertical porous enclosure, J. Fluid Mech. 368 (1998) 263–289.

[12] Nield D.A., Onset of thermohaline convection in a porous medium, Water Resour. Res. 4 (13) (1968) 553–560.

[13] Trevisan O.V., Bejan A., Mass and heat transfer by high Rayleigh number convection in a porous medium heated from below, Int. J. Heat Mass Tran. 30 (1987) 2341–2356.

[14] Murray B.T., Chen C.F., Double-diffusive convection in a porous medium, J. Fluid Mech. 201 (1989) 147–166.

[15] Chen F., Chen C.F., Double-diffusive fingering convection in a porous medium, Int. J. Heat Mass Tran. 36 (1993) 793–807.

[16] Bergman T.B., Ungan A., A note on lateral heating in a double-diffusive system, J. Fluid Mech. 194 (1988) 175–186.

[17] Kranenborg E.J., Dijkstra H.A., The structure of linearly stable double-diffusive flow patterns in a laterally heated stratified liquid, Phys. Fluids 7 (1995) 680–682.

[18] Tsitverblit N., Bifurcation phenomena in confined thermosolutal convection with lateral heating: Commencement of the double-diffusive region, Phys. Fluids 7 (1995) 718–734.

[19] Dijkstra H.A., Kranenborg E.J., A bifurcation study of double diffusive flows in a laterally heated stably stratified liquid layer, Int. J. Heat Mass Tran. 39 (1996) 2699–2710.

[20] Lauriat G., Prasad V., Natural convection in a vertical porous cavity: A numerical study for Brinkman-extended Darcy formulation, J. Heat Tran. 109 (1987) 273–299.